Food Control 79 (2017) 258–265

Contents lists available at ScienceDirect

Food Control

journal homepage: www.elsevier.com/locate/foodcont

Ultra-sensitive lab-on-a-chip detection of Sudan I in food using plasmonics-enhanced diatomaceous thin film

Xianming Kong, Kenny Squire, Xinyuan Chong, Alan X. Wang*

School of Electrical Engineering and Computer Science, Oregon State University, Corvallis, OR, 97331, USA

ARTICLE INFO

Article history:
Received 31 January 2017
Received in revised form
4 April 2017
Accepted 5 April 2017
Available online 8 April 2017

Keywords:
Sudan I
Lab on chip
Thin layer chromatography
Surface-enhanced Raman scattering
Photonic crystals
Food product

ABSTRACT

Sudan I is a carcinogenic compound containing an azo group that has been illegally utilized as an adulterant in food products to impart a bright red color to foods. In this paper, we develop a facile lab-on-a-chip device for instant, ultra-sensitive detection of Sudan I from real food samples using plasmonics-enhanced diatomaceous thin film, which can simultaneously perform on-chip separation using thin layer chromatography (TLC) and highly specific sensing using surface-enhanced Raman scattering (SERS) spectroscopy. Diatomite is a kind of nature-created photonic crystal biosilica with periodic pores and was used both as the stationary phase of the TLC plate and photonic crystals to enhance the SERS sensitivity. The on-chip chromatography capability of the TLC plate was verified by isolating Sudan I in a mixture solution containing Rhodamine 6G, while SERS sensing was achieved by spraying gold colloidal nanoparticles into the sensing spot. Such plasmonics-enhanced diatomaceous film can effectively detect Sudan I with more than 10 times improvement of the Raman signal intensity than commercial silica gel TLC plates. We applied this lab-on-a-chip device for real food samples and successfully detected Sudan I in chili sauce and chili oil down to 1 ppm, or 0.5 ng/spot. This on-chip TLC-SERS biosensor based on diatomite biosilica can function as a cost-effective, ultra-sensitive, and reliable technology for screening Sudan I and many other illicit ingredients to enhance food safety.

1. Introduction

In recent decades, there is a growing concern with regards to food safety because foodborne diseases are responsible for the majority of mortality and morbidity worldwide with nearly 30% of the population in industrialized countries suffering from foodborne illness annually (Rahman, Khan, & Oh, 2016; Woh, Thong, Behnke, Lewis, & Zain, 2016). This concern has been highlighted by scandals of illegally adding melamine to dairy products to falsely increase the protein content in China, which affected thousands of children and many of them suffered kidney damages (Chan, Griffiths, & Chan, 2008; Kong & Du, 2011). Each year, nearly 48 million people in the United States suffer from foodborne illnesses, and 128,000 are hospitalized and almost 3000 die from foodborne related diseases (Woh et al., 2016). The consumption of food contaminated with toxic ingredients can result in foodborne illnesses, thus the detection of toxic ingredients in food product is important to enhance food safety.

Sudan I is a carcinogenic compound with an azo group that is commonly used as an industrial dye, such as in dyeing plastics, oil paint, waxes, and printing. Sudan I also has been illegally utilized as an adulterant in food stuffs and cosmetics for imparting a bright red color. In April 2003, Sudan I was detected in chili products made from India and Pakistan by a French agency (Di Donna, Maiuolo, Mazzotti, De Luca, & Sindona, 2004). Sudan dyes can damage DNA, RNA, and some enzymes in the human body. Thus, Sudan dyes have been classified as carcinogenic and mutagenic compounds by International Agency for Research on Cancer (Ahmed Refat et al., 2008; Cheung, Shadi, Xu, & Goodacre, 2010). This makes it illegal to be used as a food additive according to the U.S. Food and Drug Administration (FDA) and European framework (Union, 2005). For practical purposes, instant, ultra-sensitive, and cost-effective detection of Sudan I is of high significance to ensure food safety. Numerous techniques have been employed to identify Sudan I dye in food products, most of which involve the use of chromatographic methods coupled with various detectors (Calbiani et al., 2004; He, Su, Shen, Zeng, & Liu, 2007; Rebane, Leito, Yurchenko, & Herodes, 2010). Several standard procedures of sample preprocessing are indispensable for chromatographic approaches. Sampling is usually

* Corresponding author.
E-mail address: wang@eecs.oregonstate.edu (A.X. Wang).

http://dx.doi.org/10.1016/j.foodcont.2017.04.007
0956-7135/

achieved by solvent extraction based on organic solvents such as acetone, acetonitrile or methanol. This step is, in many cases, followed by an additional cleaning and derivatization, which is time consuming and requires skilled personnel (Ostrea, 1999; Zhang, Wang, Wu, Pei, Chen, & Cui, 2014).

Thin layer chromatography (TLC) is a simple, fast and cost-effective technique for analyte separation, and can play pivotal roles for on-site sensing. Generally, after spotting samples onto the TLC plate and developing in the eluent via capillary force, the separated sample spots are visualized by the optical absorbance or fluorescence and the corresponding components are distinguished by their characteristic colors combined with different retention factor (Rf) values. However, most of the colorimetric methods used for TLC plates lack specificity and sensitivity. Routine spectroscopic technologies like Fourier Transform Infrared Spectroscopy (FT-IR) (Causin et al., 2008), mass spectroscopy (MS) (Wilson, 1999) and Surface-enhanced Raman scattering (SERS) (Zhang, Liu, Liu, Sun, & Wei, 2014) are needed to further characterize the targets. SERS spectroscopy has attained considerable interests as a sensitive and nondestructive detection method for the highly selective and sensitive detection of various analytes (X. Kong et al., 2016; Luo, Huang, Lai, Rasco, & Fan, 2016). The combination of SERS with TLC (TLC-SERS) is very promising in numerous applications due to its high throughput and sensitivity and it requires no complicated sample preprocessing (Lai, Chakravarty, Wang, Lin, & Chen, 2011). Since the pioneering work of TLC-SERS was reported by Zeiss's group (Hezel & Zeiss, 1977), this method has been successfully applied to the separation and identification of analytes from mixture samples. Examples include on-site monitoring of the aromatic pollutants in environmental water samples (Li et al., 2011), rapid identification of harmful pigments in food products, and detecting adulterants in botanical dietary supplements (Lv et al., 2015). The performance of the TLC technology is mainly dependent on the chromatographic materials and eluents. So far, most reported TLC-SERS methods use commercially available TLC plates such as silica gel or cellulose as the stationary phase, which have enabled short separation time and higher resolution. Nevertheless, the sensitivity of SERS spectroscopy from TLC plates is far from sufficient for food safety.

Diatomite consists of fossilized remains of diatom, a type of hard-shelled algae. As a kind of natural photonic biosilica from geological deposits, it has a variety of unique properties including a highly porous structure, excellent adsorption capacity, and low cost. In addition, the two dimensional (2-D) periodic pores on diatomite earth with hierarchical nanoscale photonic crystal features can provide additional enhancement for SERS sensing (Gordon, Sinton, Kavanagh, & Brolo, 2008; Ren, Campbell, Rorrer, & Wang, 2014). Herein, we fabricate TLC plates from diatomite as the stationary phase, and combine them with Au NPs to separate and identify Sudan I from real food samples (chili powder and chili sauce). The lab-on-a-chip TLC-SERS device using plasmonics-enhanced diatomaceous film demonstrated in this paper is able to detect Sudan I with nearly 10 times improvement of the intensity of Raman signals than commercially available silica gel TLC plates. It successfully detected Sudan I in chili sauce with ultra-high sensitivity down to 1 ppm.

2. Materials and methods

2.1. Materials and reagents

Tetrachloroauric acid ($HAuCl_4$) was purchased from Alfa Aesar. Trisodium citrate ($Na_3C_6H_5O_7$), cyclohexane, acetone and acetate were purchased from Macron. Diatomite (Celite209) and Sudan I were obtained from Sigma-Aldrich. Rhodamine6G (R6G) was purchased from Tokyo Chemical Industry. The food products (chili powder, chili sauce, chili oil and food oil) were purchased from local supermarkets. The chemical reagents used were of analytical grade. Water used in all experiments was deionized and further purified by a Millipore Synergy UV Unit to a resistivity of ~18.2 MΩ cm.

2.2. Preparation of Au NPs

All glassware used in the Au NP prepare process was cleaned with aqua regia (HNO_3/HCl, 1:3, v/v) followed by washing thoroughly with Milli-Q water. Au NPs with an average diameter of 60 nm were prepared using sodium citrate as the reducing and stabilizing agent according to the literature with minor modification (Grabar, Freeman, Hommer, & Natan, 1995). Briefly, a total of 50 mL of 1 mM chloroauric acid aqueous solution was heated to boil under vigorous stirring. After adding 2.1 mL of 1% trisodium citrate, the pale yellow solution turned fuchsia within several minutes. The colloids were kept under refluxing for another 15 min to ensure complete reduction of Au ions followed by cooling to room temperature.

2.3. Fabrication of diatomite earth TLC plates

The diatomaceous earth plates for TLC were fabricated by spin coating diatomite on glass slides. The diatomite biosilica was dried at 150 °C for 6 h in an oven before spreading on the glass slides. After cooling to room temperature, 11.55 g of diatomaceous earth was first dispersed in 20 mL of 0.5% aqueous solution of carboxymethyl cellulose and then transferred onto the glass slide for spin coating at 1200 rpm for 20 s. The plates were placed in the shade to dry and then annealed at 110 °C for 3 h to improve the adhesion of diatomaceous earth to the glass slides.

2.4. TLC-SERS method

The TLC-SERS method was designed for on-site detection of analytes from mixtures or real food samples as shown in Scheme 1. First, 0.5 μL liquid sample was spotted at 12 mm from the edge of the TLC plate. After drying in air, the TLC plate was kept in the TLC development chamber with mobile phase eluent (Cyclohexane and ethyl acetate v/v = 6:1). After separation of the analytes, the TLC plates were then dried in air. The Rf of the analytes on TLC plates were calculated and marked on the TLC plates so that the analyte spots could be traced even when they are invisible at low concentrations. Then 2 μL concentrated Au NPs were deposited directly three times. A Horiba Jobin Yvon Lab Ram HR800 Raman microscope equipped with a CCD detector was used to acquire the SERS spectra, and a 50× objective lens was used to focus the laser onto the SERS substrates. The excitation wavelength was 785 nm, and the laser spot size was 2 μm in diameter. The confocal pinhole was set to a diameter of 200 μm. SERS mapping images were recorded with a 20 × 20-point array. They were collected using the DuoScan module with a 2.0 μm step size, 0.5 s accumulation time, and collected in the Raman spectral range from 800 cm^{-1} to 1800 cm^{-1}. The acquired data was processed with Horiba LabSpec 5 software. The data were analyzed and processed by OriginPro2016.

2.5. Other instruments

UV–vis absorption spectra were recorded by a NanoDrop 2000 UV–Vis spectrophotometer (Thermo Scientific) using polystyrene cells of 1 cm optical path. Scanning electron microscopy (SEM) images were acquired on FEI Quanta 600 FEG SEM with 15–30 kV accelerating voltage. The microscopy images were acquired on the Horiba Jobin Yvon Lab Ram HR800 Raman microscope with a 100×

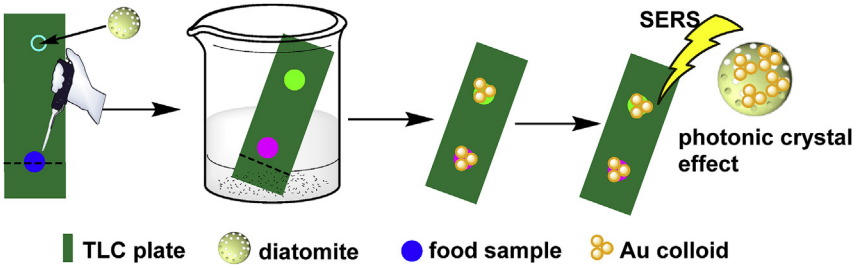

Scheme 1. Schematic representation of the TLC-SERS detection of target molecule from food product base on diatomite TLC plate.

objective lens.

3. Results and discussion

3.1. Microstructures of the diatomite TLC plate

The morphology of the diatomite biosilica used in our experiment was characterized by SEM and microscopy images (Fig. 1). The periodic pore structure of diatomite with sub-micron diameters (Fig. 1(a)) enables guided-mode resonances (GMRs) of photonic crystals (De Stefano et al., 2009), which is similar to the diatom biosilica as we reported previously (X. Kong et al., 2016). In order to verify the photonic crystal effect of diatomite, the optical image of a single diatom frustule from the diatomite was presented in Fig. 1 (b). The regular light pattern comes from the high order diffraction of the photonic crystals, which agrees with the research from Tommasi et al. (De Tommasi et al., 2010). Therefore, the diatomite used for TLC plates provides certain photonic crystal effects, although not perfect. The main component of the stationary phase on diatomite TLC plate is disk-shaped diatomite biosilica (Fig. 1 c). The size distribution of the diatomite ranges from 20 to 30 μm. The thickness of the diatomite layer on glass slides was monitored by optical microscopy as shown in Fig. 1(d). The thickness of the stationary phase on diatomite TLC plate was nearly 20 μm. Compared with commercial silica-gel TLC plates, the highly nanoporous structure and more uniform pore size of diatomite has lower fluid flow resistance (Tennikov, Gazdina, Tennikova, & Svec, 1998), which enables more homogenous fluid flows into the pores of diatomite. Therefore, the eluent migrates more smoothly and uniformly on the surface of the stationary phase during the TLC development.

3.2. Synthesis of Au colloid

SEM and UV–vis spectroscopy were employed to characterize the morphology and properties of the prepared Au NPs. The SEM images (Fig. S1) indicate that the Au NPs have a spherical shape with uniform size distribution and their diameters are estimated to be 50–60 nm. The pH of Au colloid was 6.5 and the UV–vis spectra of colloidal Au NP suspensions were shown in Fig. S2. The wavelength and intensity of the maximum absorption of the metallic

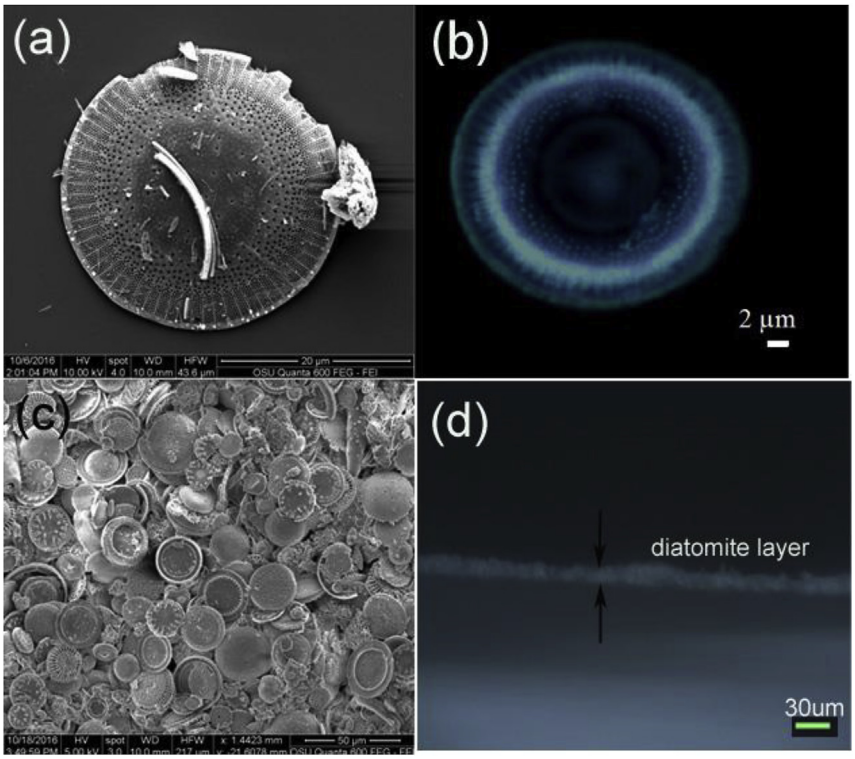

Fig. 1. SEM image of the diatomite biosilica with honeycomb structure (a), optical image of a single diatom under the microscope, showing the diffraction pattern from photonic crystals (b), SEM image of diatomite layer formed on the glass substrate (c) and the thickness of the diatomite layer (d).

NPs depends on the size, shape, concentration and surrounding dielectric environment around the nanoparticles. The localized surface plasmon resonances (LSPR) peak of the prepared Au colloids is located at 549 nm. These values correspond to relatively uniform, mono-dispersed Au colloids with diameters of approximately 50–60 nm. The concentration of Au NPs was calculated to be approximately 0.8×10^{-10} M, which is estimated using the basis of the Lambert's law base on UV–vis spectroscopy (Fig. S2) with a molar extinction coefficient of 3.4×10^{10} M^{-1} cm^{-1} (Navarro & Werts, 2013).

3.3. SERS of Sudan I from mixtures

We first investigated the potential of using SERS to detect R6G, Sudan I and their mixture. Briefly the R6G, Sudan I and the mixture (R6G and Sudan I 1/1) were mixed with Au colloid respectively, and then the SERS spectra were collected. Fig. 2(a) shows the SERS spectra of R6G, Sudan I and their mixture. The chemical structure of R6G and Sudan I were shown as Fig. 2(d). R6G is the most commonly used Raman probe molecule because of its affinity with metallic surfaces and intense Raman signals. The peak at 1308 cm^{-1} is assigned to C-O-C stretching vibrations of R6G, while the peaks at 1194, 1360 and 1508 cm^{-1} are associated with aromatic C-C stretching vibrations of R6G (X.-M. Kong et al., 2015). For Sudan I, the peak at 1160 cm^{-1} is assigned to the vibration of benzene ring with double benzene nucleus, and the peak at 1577 cm^{-1} is assigned to the vibration of azo and double benzene nucleus. The prominent peak at around 1226 cm^{-1} due to the stretching of double benzene ring and the C-H in-plane bending of phenyl groups (Pei et al., 2015; Zhang, Zhang, & Fang, 2007) was used as the feature Raman peak of Sudan I in detection. For the mixture (R6G and Sudan I 1/1), only feature peaks of R6G were observed due to the fact that the metallic surface was almost entirely covered by R6G. The NH group of R6G can easily be bound to the surface of Au NPs, while the adsorption between Sudan I and Au NPs was weak due to the hydrophobic property of Sudan I. It is hard to distinguish the Raman peak of Sudan I from the mixture by normal SERS without separation technology.

The chromatography performance of the diatomite TLC plates was evaluated using the mixture. A mixture of cyclohexane and ethyl acetate (v/v = 6:1) was used as the eluent for the separation of Sudan I from the mixture. After separation, the separated analyte spots were visualized through their own color. Sudan I travels at a faster speed and is located further from the original dropping points because of the lower molecular polarity compared with R6G. The Rf (equal to the ratio of the distance migrated by the target analyte and the solvent on the TLC plate) values of the Sudan I and R6G are 0.9 and 0 respectively. After depositing Au NPs on the corresponding spots, the SERS spectra at different spots were measured on the diatomite earth plate after the TLC separation as shown in Fig. 2. The feature peaks of Sudan I at 1226 cm^{-1} was clearly observed, which means that the diatomite earth plate can successfully separate Sudan I from the mixture. In Fig. 2, all the characteristic bands of R6G and Sudan I exhibited monotonous decrease in intensity as the mixture concentration decreases.

Mapping images of the Raman signals visualized the distribution of the analytes on the TLC plates as shown in Fig. 3. We compared the SERS spectra obtained from the diatomite TLC plates with commercial silica gel TLC plates. Fig. 3 (a) and (b) shows the Raman mapping images of 100 ppm of Sudan I on the prepared diatomite plate and the commercial TLC plate, respectively. The SERS mapping images were recorded using the integrated peak

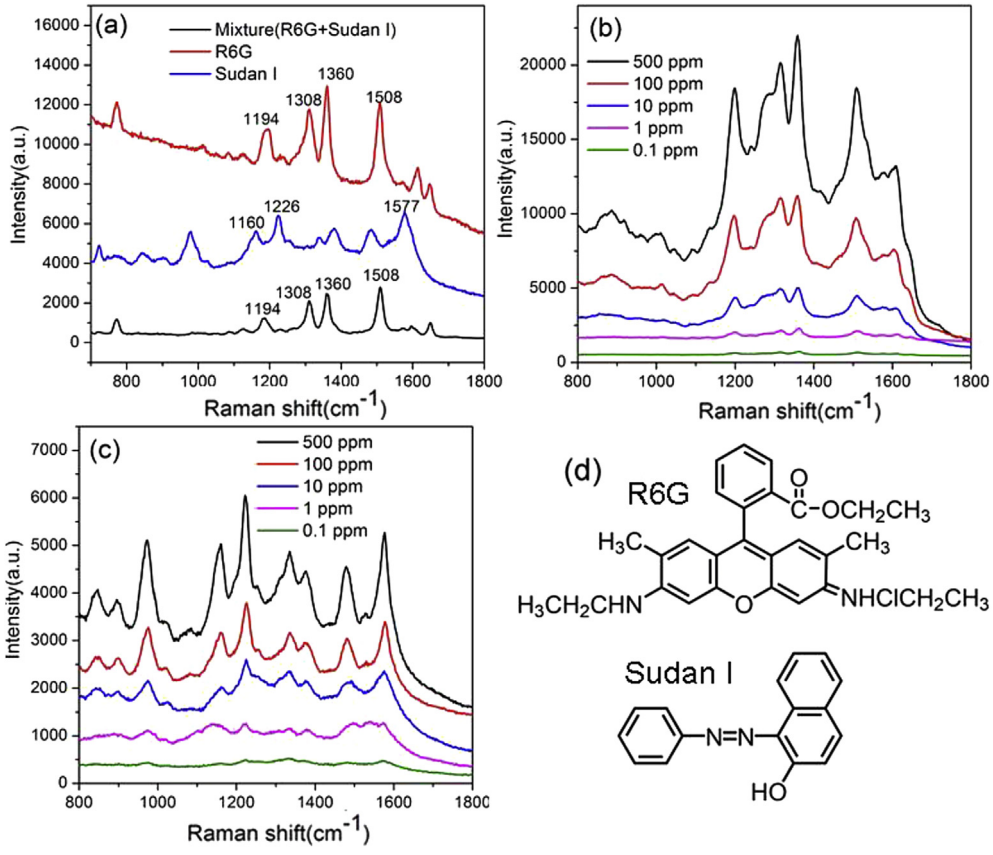

Fig. 2. SERS spectra of different samples (a) and R6G (b), Sudan I(c) separated from their mixture by diatomite TLC plate, and the chemical structure of R6G and Sudan I (d).

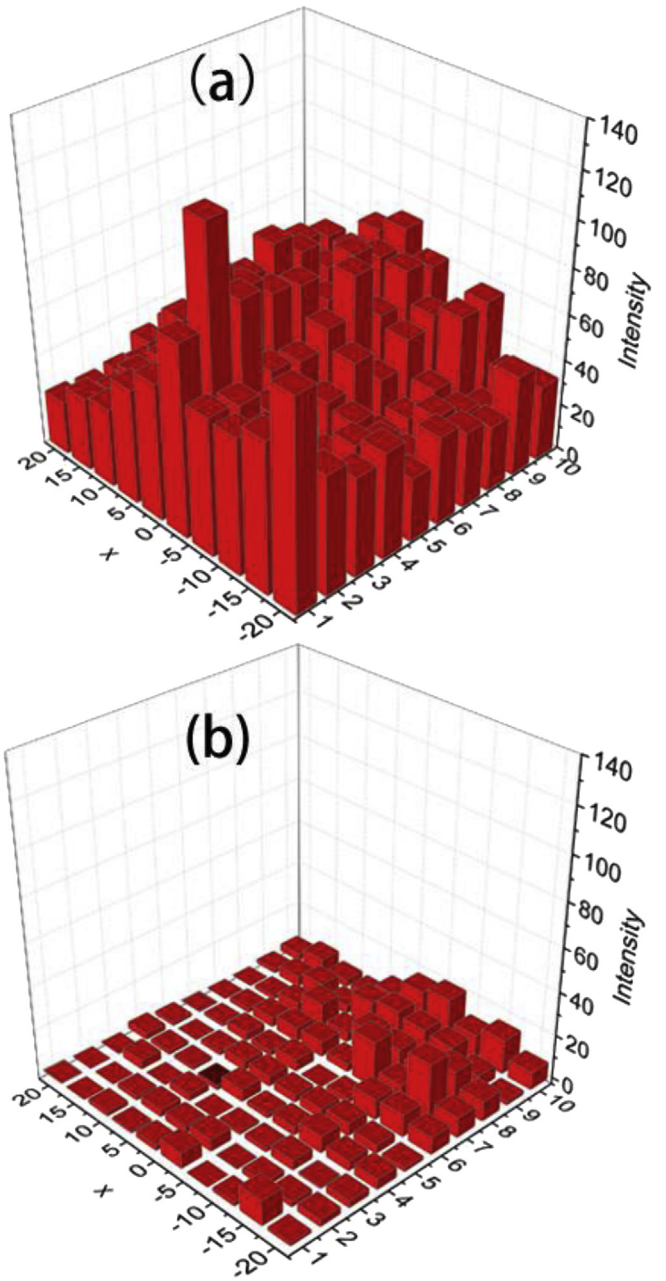

Fig. 3. Raman mapping images of 100 ppm Sudan I on (a) diatomaceous earth and (b) silica gel TLC plate.

intensity at 1220-1230 cm^{-1}. The mean value of the intensity of the featured Sudan I band at 1226 cm^{-1} is 48 and 5 for diatomite and silica gel plate, respectively. The experimental results demonstrate nearly 10 times improvement of intensity using the diatomite TLC plate compared to commercial silica gel TLC plates. The improvement was attributed to two aspects: First, in most TLC-SERS methods, the plasmonic nanoparticles are drop-casted onto the analyte spots after TLC separation. The SERS spectra collected from corresponding spot will only arise from the analytes located at the surface of the TLC plate. The thinner diatomite layer will provide higher analyte concentration at the surface of the TLC plate. The thickness of the diatomite TLC plates fabricated by spin coating is around 20 μm, which is only one third of the thickness of the commercial silica-gel TLC plate (60 μm Fig. S3). Second, the two dimensional (2-D) periodic pores on diatomite disks possess hierarchical nanoscale photonic crystal features (De Stefano et al., 2009; Fuhrmann, Landwehr, El Rharbi-Kucki, & Sumper, 2004). The hybrid photonic-plasmonic resonance modes could be formed when Au NPs are near the surface of diatomite, which will further increase the local optical field of Au NPs. Therefore, additional SERS enhancement can be achieved. The variation of the SERS intensity on TLC plate was represented by the coefficient of variation (CV = standard deviation/mean), which is 0.4 on diatomite plate and 0.9 on silica gel plate, respectively. The reproducibility of the diatom SERS substrate is much better than commercial silica gel TLC plate. The highly uniform and porous structure of the diatomite has lower flow resistance (Tennikov et al., 1998), which enables more homogenous liquid flows through the pores of diatomite. Therefore, the eluent migrates smoothly and uniformly on the surface of the stationary phase during the TLC development. For the commercial silica gel TLC plate used in the control experiment, the liquid flow mainly migrates through the gaps of the silica particles, and the analyte molecules can only stay in the inter-particle regions.

3.4. TLC-SERS analysis of Sudan I in chili products

The diatomite TLC-SERS method was used to detect Sudan I in chili products in order to demonstrate its engineering potential for on-site food analysis. Chili powder, which is a natural constituent of chili, was chosen as the target sample. 10 μL acetone was added into 10 mg chili powder with artificially added Sudan I (0.01%) because Sudan dyes can be easily dissolved in acetone, and then a 0.5 μL liquid sample was spotted onto the TLC plate for detecting Sudan I from the chili powder. During the TLC separation process, the Sudan I was separated from other components such as carotene, citric acid, capsaicin, grease and so on of chili as they have different polarities. After the TLC separation, the SERS spectra on the diatomite plate were collected. Fig. 4 (a) shows the SERS spectra of Sudan I separated from chili powder. The feature bands of Sudan I were observed at the far spot from the bottom of diatomite TLC plate, and there were no Raman signals obtained at the initial spot. No obvious Raman peaks were observed after TLC separation for chili powder without Sudan I. There were no Raman signals of Sudan I observed by directly measuring the chili powder without TLC separation either (Fig. S4). Chili sauce is another chili product that is commonly consumed. Salt, vinegar and other types of fruits or vegetables sauces are usually added as ingredients for chili sauce, which makes it difficult to detect Sudan I from chili sauce by SERS. Here we used this TLC-SERS method for on-chip detection of Sudan I from chili sauce. SERS spectra of Sudan I from chili sauce are shown in Fig. 4(b), and the location of the characteristic peaks is the same as that from chili powder. Simple linear regression was used to correlate the linear relationship between the Raman intensity of the characteristic peak and the logarithm concentration of Sudan I in chili sauce as shown in Fig. 4(c). The coefficient of determination (R^2) is 0.9. The detection limit, which is defined as the signal-to-noise (SNR) ratio of 3 (Lou et al., 2011) as marked by the red line in Fig. 4 (c), is determined to be lower than 1 ppm (0.5 ng/spot). In order to view the featured Raman peak clearly, the second derivative transformation method of the SERS spectra was employed (Luo et al., 2016). The Raman spectra of Sudan I in chili sauce were smoothed under first polynomial subtraction. The second derivative transformation of the peak at 1226 cm^{-1} is shown in Fig. 4 (d). The slight shift of the peak values at different concentrations might come from the smoothing process of the Raman spectra. As the concentration of Sudan I increase from 1 to 1000 ppm, the second derivative of Raman intensity over the wavenumber at 1226 cm^{-1} increases as well.

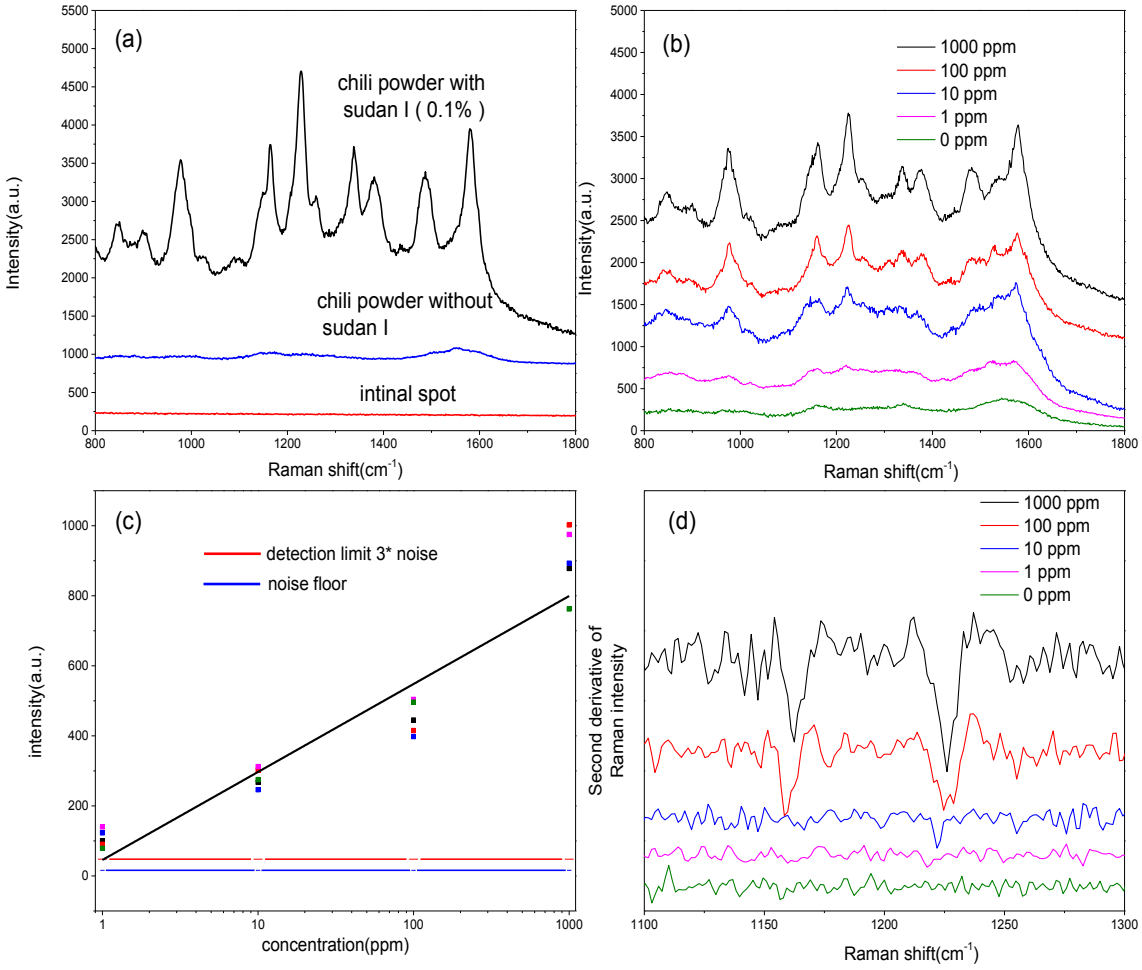

Fig. 4. SERS spectra of Sudan I from chili powder (a) and chili sauce (b) on diatomite plate after TLC separation, (c) SERS intensity as a function of logarithm of Sudan I concentration in chili sauce and (d) second derivative transformation of a SERS spectra at 1226 cm^{-1} for different concentrations of Sudan I in chili sauce, and the detection limit was indicated as the red line in (c). (For interpretation of the references to colour in this figure legend, the reader is referred to the web version of this article.)

3.5. TLC-SERS monitor Sudan I from chili oil

When Sudan I was used as an adulterant in cooking oil, the appearance of that oil was similar to chili oil as shown in Fig. 5(a). Among the procedures for metallic nanoparticles preparation, those that require an aqueous media are the most convenient because of water's ability to solubilize a variety of ions and stabilizing agents (Wei, Yang, Lee, Yang, & Wang, 2004). But unfortunately, phase separation would happen as the hydrophilic Au colloids mix with oil as shown in Fig. 5(a). The two phase oil–aqueous colloid prevented the adsorption of analytes to the Au NPs due to the localization of Sudan I within oil droplets, which makes it difficult to acquire the SERS spectra from oil phase as shown in Fig. S5. Usually an extraction process is needed before detecting analytes in oil sample. The metallic nanoparticles with hydrophobic surfaces could be dispersed in oil phase, but the transfer of the nanoparticles from aqueous to organic phase or preparation of metallic nanoparticle with surfactant is indispensable. TLC is a kind of simple, fast and cost-effective separation technology, which have been successfully used for separating analytes from oil and petroleum samples (Cercaci, Rodriguez-Estrada, & Lercker, 2003; Pollard et al., 1992). The diatomite base TLC-SERS method was employed to detect Sudan I from an oil sample in this work. The chili oil with different concentrations of Sudan I was directly dispensed onto the diatomite TLC plate. After separation, the SERS spectra were obtained. The SERS spectra of Sudan I separated from chili oil are shown in Fig. 5(b). Comparing to the SERS spectra of Sudan I standard solution (Fig. 2), the characteristic peaks located at around 1160 cm^{-1}, 1226 cm^{-1} and 1577 cm^{-1} for Sudan I separated from chili oil were also consistent with the SERS spectra of Sudan I standard solutions located at 1158 cm^{-1}, 1226 cm^{-1} and 1577 cm^{-1} but with a small spectral shift. Obviously, some non-targeted ingredients from the chili oil interfered with the interaction between Sudan I molecules and the surface of Au NPs, which affected the bonding strength of the pertinent functional groups (Luo et al., 2016). The non-targeted ingredients could possibly be oil as it could migrate on the TLC plate during the developing process (Chen, Huang, & Zhao, 2015). When the concentration of Sudan I is down to 1 ppm in chili oil, the featured Raman peaks of Sudan I can still be observed.

4. Conclusion

In summary, we have developed a simple, rapid and cost-effective lab-on-a-chip device to separate and detect Sudan I from real food samples by TLC-SERS using diatomite as the stationary phase. The experimental results demonstrate nearly 10 times improvement of intensity compared to commercial silica-gel TLC plates. The improvement of intensity was attributed to the thinner chromatography layer and the periodic porous structure of

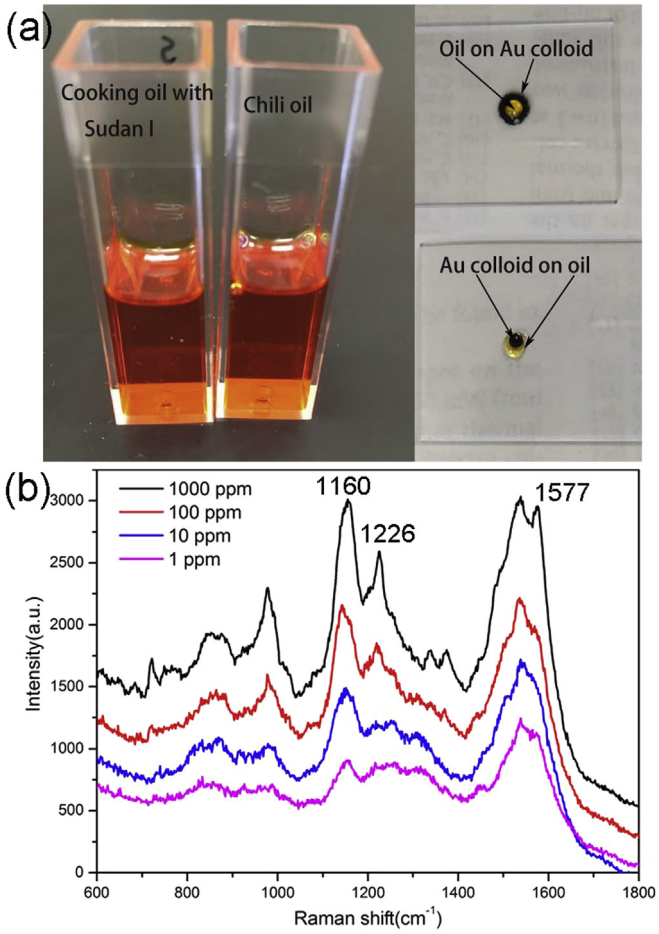

Fig. 5. (a) Photo image of oil samples and after mixed with Au colloids, (b) SERS spectra of Sudan I from chili oil.

diatomite, which can provide additional SERS enhancement due to the photonic crystal effect and homogenous porosity. This technique determined Sudan I levels in chili sauce down to 1 ppm (0.5 ng/spot) without sample preprocessing. This TLC-SERS biosensor using diatomite biosilica can be applied as a cost effective, ultrasensitive and reliable technology for screening many other illicit pigments in real food product to enhance food safety.

Acknowledgement

The authors would like to acknowledge the support from the National Institutes of Health under Grant No. 1R03EB018893 and the Oregon State University Venture Development Fund.

Appendix A. Supplementary data

Supplementary data related to this article can be found at http://dx.doi.org/10.1016/j.foodcont.2017.04.007.

References

Ahmed Refat, N. A., Ibrahim, Z. S., Moustafa, G. G., Sakamoto, K. Q., Ishizuka, M., & Fujita, S. (2008). The induction of cytochrome P450 1A1 by Sudan dyes. *Journal of Biochemical and Molecular Toxicology, 22*(2), 77–84.

Calbiani, F., Careri, M., Elviri, L., Mangia, A., Pistara, L., & Zagnoni, I. (2004). Development and in-house validation of a liquid chromatography–electrospray–tandem mass spectrometry method for the simultaneous determination of Sudan I, Sudan II, Sudan III and Sudan IV in hot chilli products. *Journal of Chromatography A, 1042*(1), 123–130.

Causin, V., Casamassima, R., Marega, C., Maida, P., Schiavone, S., Marigo, A., et al. (2008). The discrimination potential of ultraviolet-visible spectrophotometry, thin layer chromatography, and fourier Transform infrared spectroscopy for the forensic analysis of black and blue ballpoint inks. *Journal of Forensic Sciences, 53*(6), 1468–1473.

Cercaci, L., Rodriguez-Estrada, M. T., & Lercker, G. (2003). Solid-phase extraction–thin-layer chromatography–gas chromatography method for the detection of hazelnut oil in olive oils by determination of esterified sterols. *Journal of Chromatography A, 985*(1), 211–220.

Chan, E., Griffiths, S., & Chan, C. (2008). Public-health risks of melamine in milk products. *The Lancet, 372*(9648), 1444–1445.

Chen, J., Huang, Y.-w., & Zhao, Y. (2015). Detection of polycyclic aromatic hydrocarbons from cooking oil using ultra-thin layer chromatography and surface enhanced Raman spectroscopy. *Journal of Materials Chemistry B, 3*(9), 1898–1906.

Cheung, W., Shadi, I. T., Xu, Y., & Goodacre, R. (2010). Quantitative analysis of the banned food dye Sudan-1 using surface enhanced Raman scattering with multivariate chemometrics. *The Journal of Physical Chemistry C, 114*(16), 7285–7290.

De Stefano, L., Maddalena, P., Moretti, L., Rea, I., Rendina, I., De Tommasi, E., et al. (2009). Nano-biosilica from marine diatoms: A brand new material for photonic applications. *Superlattices and Microstructures, 46*(1), 84–89.

De Tommasi, E., Rea, I., Mocella, V., Moretti, L., De Stefano, M., Rendina, I., et al. (2010). Multi-wavelength study of light transmitted through a single marine centric diatom. *Optics Express, 18*(12), 12203–12212.

Di Donna, L., Maiuolo, L., Mazzotti, F., De Luca, D., & Sindona, G. (2004). Assay of Sudan I contamination of foodstuff by atmospheric pressure chemical ionization tandem mass spectrometry and isotope dilution. *Analytical Chemistry, 76*(17), 5104–5108.

Fuhrmann, T., Landwehr, S., El Rharbi-Kucki, M., & Sumper, M. (2004). Diatoms as living photonic crystals. *Applied Physics B, 78*(3–4), 257–260.

Gordon, R., Sinton, D., Kavanagh, K. L., & Brolo, A. G. (2008). A new generation of sensors based on extraordinary optical transmission. *Accounts of Chemical Research, 41*(8), 1049–1057.

Grabar, K. C., Freeman, R. G., Hommer, M. B., & Natan, M. J. (1995). Preparation and characterization of Au colloid monolayers. *Analytical Chemistry, 67*(4), 735–743.

He, L., Su, Y., Shen, X., Zeng, Z., & Liu, Y. (2007). Determination of Sudan dye residues in eggs by liquid chromatography and gas chromatography–mass spectrometry. *Analytica Chimica Acta, 594*(1), 139–146.

Hezel, U. B., & Zeiss, C. (1977). Potential and experience in quantitative "high performance thin-layer chromatography" HPTLC. *Journal of Chromatography Library, 9*, 147–188.

Kong, X., & Du, X. (2011). In situ IRRAS studies of molecular recognition of barbituric acid lipids to melamine at the air–water interface. *The Journal of Physical Chemistry B, 115*(45), 13191–13198.

Kong, X.-M., Reza, M., Ma, Y.-B., Hinestroza, J.-P., Ahvenniemi, E., & Vuorinen, T. (2015). Assembly of metal nanoparticles on regenerated fibers from wood sawdust and de-inked pulp: Flexible substrates for surface enhanced Raman scattering (SERS) applications. *Cellulose, 22*(6), 3645–3655.

Kong, X., Xi, Y., LeDuff, P., Li, E., Liu, Y., Cheng, L.-J., et al. (2016). Optofluidic sensing from inkjet-printed droplets: The enormous enhancement by evaporation-induced spontaneous flow on photonic crystal biosilica. *Nanoscale, 8*(39), 17285–17294.

Lai, W.-C., Chakravarty, S., Wang, X., Lin, C., & Chen, R. T. (2011). Photonic crystal slot waveguide absorption spectrometer for on-chip near-infrared spectroscopy of xylene in water. *Applied Physics Letters, 98*(2), 023304.

Li, D., Qu, L., Zhai, W., Xue, J., Fossey, J. S., & Long, Y. (2011). Facile on-site detection of substituted aromatic pollutants in water using thin layer chromatography combined with surface-enhanced Raman spectroscopy. *Environmental Science & Technology, 45*(9), 4046–4052.

Lou, T., Wang, Y., Li, J., Peng, H., Xiong, H., & Chen, L. (2011). Rapid detection of melamine with 4-mercaptopyridine-modified gold nanoparticles by surface-enhanced Raman scattering. *Analytical and Bioanalytical Chemistry, 401*(1), 333–338.

Luo, H., Huang, Y., Lai, K., Rasco, B. A., & Fan, Y. (2016). Surface-enhanced Raman spectroscopy coupled with gold nanoparticles for rapid detection of phosmet and thiabendazole residues in apples. *Food Control, 68*, 229–235.

Lv, D., Cao, Y., Lou, Z., Li, S., Chen, X., Chai, Y., et al. (2015). Rapid on-site detection of ephedrine and its analogues used as adulterants in slimming dietary supplements by TLC-SERS. *Analytical and Bioanalytical Chemistry, 407*(5), 1313–1325.

Navarro, J. R., & Werts, M. H. (2013). Resonant light scattering spectroscopy of gold, silver and gold–silver alloy nanoparticles and optical detection in microfluidic channels. *Analyst, 138*(2), 583–592.

Ostrea, E. M. (1999). Testing for exposure to illicit drugs and other agents in the neonate: A review of laboratory methods and the role of meconium analysis. *Current Problems in Pediatrics, 29*(2), 41–56.

Pei, L., Ou, Y., Yu, W., Fan, Y., Huang, Y., & Lai, K. (2015). Au-Ag core-shell nanospheres for surface-enhanced Raman scattering detection of Sudan I and Sudan II in chili powder. *Journal of Nanomaterials, 16*(1), 215.

Pollard, S. J., Hrudey, S. E., Fuhr, B. J., Alex, R. F., Holloway, L. R., & Tosto, F. (1992). Hydrocarbon wastes at petroleum-and creosote-contaminated sites: Rapid characterization of component classes by thin-layer chromatography with flame ionization detection. *Environmental Science & Technology, 26*(12), 2528–2534.

Rahman, S., Khan, I., & Oh, D. H. (2016). Electrolyzed water as a novel sanitizer in the

food Industry: Current trends and future perspectives. *Comprehensive Reviews in Food Science and Food Safety, 5*(3), 471–490.
Rebane, R., Leito, I., Yurchenko, S., & Herodes, K. (2010). A review of analytical techniques for determination of Sudan I–IV dyes in food matrixes. *Journal of Chromatography A, 1217*(17), 2747–2757.
Ren, F., Campbell, J., Rorrer, G. L., & Wang, A. X. (2014). Surface-enhanced Raman spectroscopy sensors from nanobiosilica with self-assembled plasmonic nanoparticles. *Selected Topics in Quantum Electronics, IEEE Journal of, 20*(3), 127–132.
Tennikov, M. B., Gazdina, N. V., Tennikova, T. B., & Svec, F. (1998). Effect of porous structure of macroporous polymer supports on resolution in high-performance membrane chromatography of proteins. *Journal of Chromatography A, 798*(1), 55–64.
Union, E. (2005). *Commission Decision 2005/402/EC on emergency measures regarding chilli, chilli products, curcuma and palm oil* (Legislation).
Wei, G.-T., Yang, Z., Lee, C.-Y., Yang, H.-Y., & Wang, C. C. (2004). Aqueous-organic phase transfer of gold nanoparticles and gold nanorods using an ionic liquid. *Journal of the American Chemical Society, 126*(16), 5036–5037.
Wilson, I. (1999). The state of the art in thin-layer chromatography–mass spectrometry: A critical appraisal. *Journal of Chromatography A, 856*(1), 429–442.
Woh, P. Y., Thong, K. L., Behnke, J. M., Lewis, J. W., & Zain, S. N. M. (2016). Evaluation of basic knowledge on food safety and food handling practices amongst migrant food handlers in Peninsular Malaysia. *Food Control, 70*, 64–73.
Zhang, Z.-M., Liu, J.-F., Liu, R., Sun, J.-F., & Wei, G.-H. (2014). Thin layer chromatography coupled with surface-enhanced Raman scattering as a facile method for on-site quantitative monitoring of chemical reactions. *Analytical Chemistry, 86*(15), 7286–7292.
Zhang, Y., Wang, Z., Wu, L., Pei, Y., Chen, P., & Cui, Y. (2014). Rapid simultaneous detection of multi-pesticide residues on apple using SERS technique. *Analyst, 139*(20), 5148–5154.
Zhang, L., Zhang, P., & Fang, Y. (2007). Magnetron sputtering of silver nanowires using anodic aluminum oxide template: A new active substrate of surface enhanced Raman scattering and an investigation of its enhanced mechanism. *Analytica Chimica Acta, 591*(2), 214–218.